Can the MDCDW condensate withstand the heat of a cold neutron star?

W. Gyory

Department of Physics and Astronomy, University of Texas Rio Grande Valley, 1201 West University Drive, Edinburg, Texas 78539, USA
Physics Department, CUNY – The Graduate Center, 365 5th Ave, New York, New York 10016, USA

E-mail: wgyory@gradcenter.cuny.edu

Abstract. The correct description of strongly interacting matter at low temperatures and moderately high densities—in particular the conditions realized inside neutron stars—is still unknown. We review some recent results on the magnetic dual chiral density wave (MDCDW) phase, a candidate phase of quark matter for this region of the QCD phase diagram. We highlight the effects of magnetic fields and temperature on the condensate, which can be explored using a high-order Ginzburg-Landau (GL) expansion. We also explain how the condensate's nontrivial topology, which arises due to the asymmetry in the lowest Landau level modes, affects its physical properties. Finally, we comment on the possible relevance of these results to neutron star applications. Over a wide range of densities and magnetic field strengths, MDCDW is preferred over the chirally symmetric ground state at temperatures consistent with typical cold neutron stars, and in some cases, even hot ones.

1. Introduction

Quantum chromodynamics (QCD) is generally accepted as the correct theory of strong interactions, but a firm theoretical understanding of its low-energy behavior remains elusive. The high-energy regime, by contrast, is relatively well understood due to the theory's asymptotic freedom, the phenomenon in which the coupling constant becomes small at large energy scales. Perturbation theory can therefore be used to study the quark-gluon plasma (QGP) phase, which appears at extremely high temperatures and all densities, and the color-superconducting color-flavor-locked (CFL) phase, which appears at low temperatures and extremely high densities.

Meanwhile, at very low densities, lattice QCD gives reliable predictions. A confined hadronic phase is predicted at low temperatures, and at sufficiently high temperatures deconfinement occurs and the QGP phase is realized. With increasing density, however, lattice calculations become infeasible due to the so-called "numerical sign problem," which is associated with the evaluation of highly oscillatory integrals. The region of moderately high densities but very low temperatures lies outside the domains of perturbative and lattice QCD, and is hence relatively poorly understood. To investigate QCD under these conditions, theorists must turn to nonperturbative methods, such as effective theories and complex simulations.

Inhomogeneous condensates have long been a candidate of interest for this region of the QCD phase diagram. In this paper we will review some of our recent results on one such condensate, the magnetic dual chiral density wave (MDCDW), with an eye toward its possible relevance

to neutron stars (NSs). To motivate our study of MDCDW, we first review the historical background of similar inhomogeneous phases, and also explain the intuition behind why such phases may arise in dense QCD. Our brief summary is based off of [1], where more details can be found.

1.1. Historical Background

Spatially inhomogeneous phases are ubiquitous in condensed matter physics. Examples include charge and spin density waves, crystalline superconducting phases, such as the Fulde-Ferrell-Larkin-Ovchinnikov (FFLO) phase [2], and mass and spin imbalanced cold atom Fermi gases [3]. The suggestion that spatial inhomogeneity might arise in nuclear matter goes at least as far back as 1960, when Overhauser examined the possibility of density waves appearing in this context [4]. Similar ideas appeared in the 1970s and 1980s, when inhomogeneous pion condensation was investigated by Migdal and others [5].

An inhomogeneous *chiral* condensate—that is, a spatially varying condensate that spontaneously breaks the chiral symmetry of QCD—was first explored in 1992 by Deryagin, Grigoriev and Rubakov [6], who examined dense QCD in the limit of a large number of colors. Research on inhomogeneous chiral condensates continued throughout the 1990s and 2000s, when several authors analyzed these phases in the framework of specific models, such as the sigma model [7], the Nambu–Jona Lasinio (NJL) model [8], and quarkyonic matter [9]. Single-modulated inhomogeneous condensates were generally found to be preferred to those with higher-dimensional modulations and to the chirally symmetric state over a range of moderately large densities.

1.2. Pairing Mechanisms

Following [1] and [9], we offer a conceptual explanation for the appearance of spatial inhomogeneity in QCD through particle pairing mechanisms. For the sake of comparison, let us first consider the crystalline superconducting phases of condensed matter physics. In ordinary BCS theory, pairing occurs between electrons at opposite sides of the Fermi surface. These electrons have equal but opposite momenta, so they form Cooper pairs with zero total momentum, giving rise to a homogeneous condensate.

Inhomogeneity can arise when the system is placed under a condition that creates a stress between the Fermi momenta of the particles participating in the pair. For example, in a magnetic field the electrons with opposite spin have different Fermi surfaces. There is now a free energy cost associated with lifting one of the electrons to the other's Fermi surface to form a pair with zero net momentum. In this case the BCS pairing will be favored only as long as the energy cost from the stress between the Fermi surfaces is lower than the gain in condensation energy. On the other hand, it costs no free energy to excite pairs of electrons that are both near their respective Fermi surfaces and hence form a pair with nonvanishing total momentum, giving rise to an inhomogeneous condensate.

In QCD, the main particle-particle attractive channel pairs quarks of different flavors and colors. At very high densities, the Fermi surfaces of different flavors are all equal and BCS pairing is favored. With decreasing density, however, a stress emerges between the Fermi surfaces of different flavors. In close analogy to the situation described above, the BCS pairing is eventually replaced by Cooper pairing with nonzero net momentum, producing a state of crystalline color superconductivity [10].

In the case of chiral condensates, we begin by considering the QCD vacuum, in which left-handed quarks pair with right-handed antiquarks and vice versa, giving rise to a homogeneous chiral condensate $\langle\bar{\psi}\psi\rangle = \langle\bar{\psi}_L\psi_R\rangle + \langle\bar{\psi}_R\psi_L\rangle$. Introducing a large chemical potential μ gives rise to a positive quark density and therefore a Fermi surface. The quark-antiquark pairing mechanism of the vacuum now has a free energy cost of $\sim 2\mu$ required to lift an antiquark from

the Dirac sea to the Fermi surface. On the other hand, the formation of a Fermi surface opens a new possibility, where quarks near the Fermi surface can be excited with almost no energy cost and pair with holes. Because the gluon propagator is large at low energies, it is energetically favored for quarks to pair with holes of the same momentum (meaning zero relative momentum). Thus, the favored pairing mechanism is one in which the net momentum of the pair is nonzero, and hence the chiral condensate is inhomogeneous.

In each case, a pairing mechanism generates a spatial inhomogeneity in the ground state of the system, and as a consequence, the spectrum of the quasiparticles becomes dependent on the parameter that measures the inhomogeneity of the condensate. The exact form of the quasiparticle spectrum will depend on the ansatz used for the inhomogeneous chiral condensate.

2. Theory of the MDCDW Condensate

In this section, we study the MDCDW phase in the context of a three-color and two-flavor NJL model with a background magnetic field,

$$\mathcal{L} = \bar{\psi}[i\gamma^\mu(\partial_\mu + iQA_\mu) + \gamma_0\mu]\psi + G[(\bar{\psi}\psi)^2 + (\bar{\psi}i\tau\gamma_5\psi)^2]. \tag{1}$$

Here $\psi = (u,d)^T$, $Q = \mathrm{diag}(e_u, e_d) = (\frac{2}{3}e, -\frac{1}{3}e)$, μ is the quark chemical potential, G is the four-fermion coupling constant, and τ_a are the Pauli matrices acting in isospin space. A_μ is the sum of a background magnetic field $\bar{A}_\mu = (0,0,Bx,0)$ and fluctuation field $\tilde{A}_\mu$. The condensate is given by the ansatz

$$\langle\bar{\psi}\psi\rangle + i\langle\bar{\psi}i\gamma^5\tau_3\psi\rangle = \Delta e^{iqz}, \tag{2}$$

where the magnitude Δ and modulation q are the order parameters. In the following, we use the variables m and b instead of Δ and q, defined as $m = -2G\Delta$ and $b = q/2$.

Expanding (1) about (2) gives the mean-field theory of the MDCDW phase, which can be used to compute the energy modes for the lowest Landau level (LLL) and higher Landau levels (HLL),

$$\text{(LLL)} \qquad E_0 = \epsilon\sqrt{m^2+k^2} + b, \qquad \epsilon = \pm \tag{3}$$

$$\text{(HLL)} \qquad E_\ell = \epsilon\sqrt{\left(\xi\sqrt{m^2+k^2}+b\right)^2 + 2|e_f B|\ell}, \qquad \epsilon = \pm, \xi = \pm, \ell = 1,2,3,... \tag{4}$$

and the free energy,

$$\Omega = \sum_f \left[\Omega^f_{vac}(B) + \Omega^f_{anom}(B,\mu) + \Omega^f_\mu(B,\mu) + \Omega^f_T(B,\mu,T)\right] + \frac{m^2}{4G}, \tag{5}$$

$$\Omega^f_{vac} = \frac{1}{4\sqrt{\pi}}\frac{N_c\,|e_f B|}{(2\pi)^2}\int_{-\infty}^{+\infty} dk \sum_{\ell\xi\epsilon}\int_{1/\Lambda^2}^{\infty}\frac{ds}{s^{3/2}}e^{-s(E_\ell)^2} \tag{6}$$

$$\Omega^f_{anom} = -\frac{N_c\,|e_f B|}{(2\pi)^2}2b\mu \tag{7}$$

$$\Omega^f_\mu = -\frac{N_c\,|e_f B|}{(2\pi)^2}\int_{-\infty}^{+\infty} dk \sum_{\xi,\ell>0}\left[(\mu - E_\ell)\theta(\mu - E_\ell)\right]\Big|_{\epsilon=+} + \Omega^{f,LLL}_\mu \tag{8}$$

$$\Omega^{f,LLL}_\mu = -\frac{1}{2}\frac{N_c\,|e_f B|}{(2\pi)^2}\int_{-\infty}^{+\infty} dk \sum_\epsilon \left(|E_0 - \mu| - |E_0|\right)_{\mathrm{reg}} \tag{9}$$

$$\Omega^f_T = -\frac{N_c\,|e_f B|}{(2\pi)^2}\frac{1}{\beta}\int_{-\infty}^{+\infty} dk \sum_{\ell\xi\epsilon}\ln\left(1 + e^{-\beta|E_\ell - \mu|}\right). \tag{10}$$

More details on these calculations can be found in [11]. The "reg" subscript on (9) indicates that the integral should be understood as $\lim_{L\to\infty}\int_{-L}^{L} dk$. Note that the energy modes for the LLL are *not* symmetric about zero, i.e., the two modes corresponding to $\epsilon = \pm$ are not equal in magnitude with an opposite overall sign, of the form $\pm|E_0|$. This asymmetry is related to the theory's nontrivial topology, which is explored at length in [12]. The anomalous term (7) is an important consequence of this asymmetry, and it leads to several physical features of the MDCDW phase that are absent in the DCDW phase, which is given by the same ansatz but without a background magnetic field. We will present our main results and then describe how certain aspects of these results arise from the topology.

3. Results

To determine the order parameters m and b, we use two approaches. The first is direct numerical computation of (5), using optimization algorithms to search for the values that minimize the free energy. In the following, we refer to the data obtained in this way as the "exact" results. The second approach is to use a Ginzburg-Landau (GL) expansion, which results in a polynomial expression for (5) in terms of m and b that can then be minimized. We obtained important results using both methods.

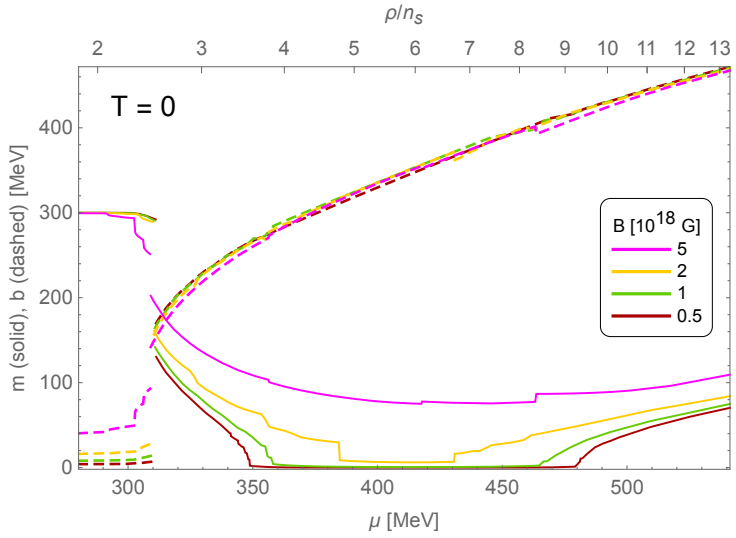

Figure 1. Order parameters m (solid) and b (dashed) plotted against chemical potential at zero temperature and various magnetic field strengths.

3.1. Zero temperature

Fig. 1 shows the exact results for m and b plotted against chemical potential at zero temperature and various magnetic fields. Observe that at any fixed value of μ in the region $\mu \gtrsim 300$ MeV, the condensate magnitude m (solid lines in Fig. 1) increases with magnetic field. For fields $B \gtrsim 2\times 10^{18}$ G, m remains large over this entire region. For smaller but nonvanishing magnetic fields, the condensate magnitude becomes small over a region of intermediate μ, but it still does not completely vanish. The behavior in this region is markedly different when no magnetic field is present, in which case m vanishes and b is undefined; physically, there can be no spatial inhomogeneity if the condensate is not present, and mathematically, we see from the ansatz (2) that no quantity can depend on b $(= q/2)$ when $m = 0$. The fact that $m \neq 0$ over the intermediate region in Fig. 1 is emphasized by the existence of b over the entire range of μ.

At very high values of μ, the condensate magnitude begins to increase again and take on sizeable values (Fig. 1, $\mu \gtrsim 450$ MeV). We also observed this behavior in the absence of a magnetic field [13]. In terms of the particle-hole pairing mechanism discussed earlier, this resurgence of the condensate magnitude can be understood as a consequence of the expanding Fermi surface with increasing μ, which provides more phase space for the particle-hole pairs to form.

Note also that in the region of smaller chemical potentials, $\mu \lesssim 300$ MeV, the modulation parameter b is small but nonzero. Though not shown in Fig. 1, this trend continues to the left, with the modulation decreasing roughly linearly with μ until vanishing at $\mu = 0$ [11]. Thus, the condensate is inhomogeneous at all finite chemical potentials, which is not the case when no magnetic field is present. This feature is a consequence of the anomalous term (7). In this region, we have $b \ll m$ and $\mu < m$, so the θ function in (8) vanishes. The HLL can only contribute to the free energy through the vacuum term, which has no μ dependence. An exact closed-form expression for the LLL medium contribution (9), given in [12], reveals that it also vanishes in this region of small μ. The anomalous term (7), however, favors b as long as $\mu > 0$. Indeed, since $\partial\Omega_{anom}/\partial b \sim -B\mu$, we see that b is favored more strongly with increasing chemical potential or magnetic field, in agreement with Fig. 1.

3.2. Finite temperature

To examine the condensate at finite temperatures, it is convenient to obtain results using a GL expansion,

$$\begin{aligned}\Omega = {} & \alpha_{2,0}m^2 + \beta_{3,1}bm^2 + \alpha_{4,0}m^4 + \alpha_{4,2}b^2m^2 + \beta_{5,1}bm^4 \\ & + \beta_{5,3}b^3m^2 + \alpha_{6,0}m^6 + \alpha_{6,2}b^2m^4 + \alpha_{6,4}b^4m^2. \end{aligned} \tag{11}$$

This expression is obtained by expanding the free energy in terms of the condensate field $M(x)$ and its derivatives ∇M, using only the structures permitted by the symmetries of the theory, and then substituting the ansatz (2) for M [14]. We use the symbol β instead of α to label the terms with odd powers of b, highlighting that these terms vanish in the absence of a magnetic field and hence contain information about the topology of MDCDW. To see this, observe that the transformation $b \to -b$ leaves the HLL contribution to (5)–(10) unchanged, due to the sum of terms with $\xi = \pm 1$ in (4). The HLL contribution to the free energy is thus an even function of b, but the β coefficients are obtained by evaluating $(\partial/\partial b)^n \Omega\big|_{b=0}$ for odd n. This argument breaks down for the LLL due to their asymmetry.

The coefficients can be found by evaluating derivatives of (5)–(10) at $m = b = 0$. Using the Euler-Maclaurin formula to approximate the Landau sums as a series of integrals, analytical expressions for the general Nth-order coefficients can be obtained; the formulas are given in (12)–(15) of [13]. It is therefore possible to obtain results using very high-order (e.g., 20th or 30th) GL expansions. The analytical expression for each coefficient contains powers of μ in the denominator so that the powers of b in (11) become powers of b/μ, which is always less than 1 and controls the convergence of the expansion. The GL expansion is especially useful for examining the condensate at finite temperature, because the numerical evaluation of (10) is computationally burdensome.

Solving for the minimum m and b using a high-order GL expansion, one finds that as temperature increases, the magnitude m decreases and eventually vanishes, indicating that the chirally symmetric ground state becomes favored over the condensate [13]. This temperature, called the critical temperature, is plotted against chemical potential in Figs. 2 and 3 at various magnetic field values. Since stronger magnetic fields increase m, they have a higher critical temperature. Also, due to the small but nonvanishing m in the region of intermediate μ (Fig. 1, 350 MeV $\lesssim \mu \lesssim$ 480 MeV), there is a corresponding small but nonvanishing critical temperature over this region, indicated with a gray box in Fig. 2 and plotted in more detail in Fig. 3.

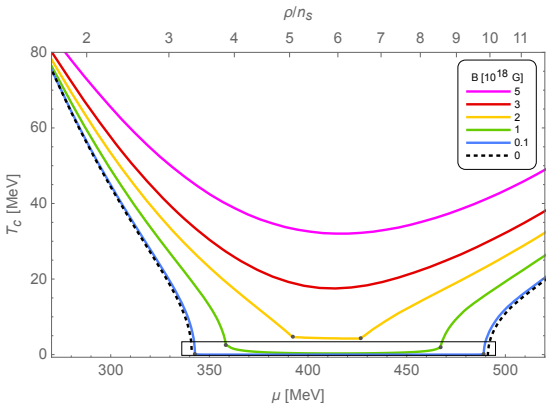

Figure 2. Critical temperature vs chemical potential at various magnetic field strengths.

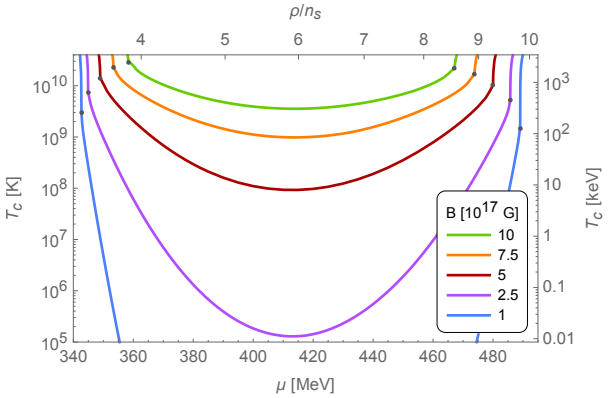

Figure 3. Zoomed-in plot of the gray box in Fig. 2, with some additional magnetic fields of order 10^{17} G. Note the logarithmic scales with different units on the left and right axes.

These results show that MDCDW is a viable candidate phase for the finite-temperature environments of neutron stars. Note that the temperature scale of Fig. 2 is on the order of MeV, whereas typical cold NS temperatures are on the order of keV. Only in the region of intermediate μ, corresponding to densities of about 4–10 times nuclear saturation density n_s (see upper axes of Figs. 2 and 3), does the critical temperature drop to the keV scale, and even then MDCDW can exist at all densities in magnetic fields $B \gtrsim 5 \times 10^{17}$ G. For example, we see in Fig. 3 that the critical temperature in a magnetic field of 5×10^{17} G (dark red curve) reaches a minimum value of about 10 keV (right axis), so an NS at any temperature below 10 keV could host MDCDW over the entire range of densities shown here. For stronger magnetic fields, at least a few times 10^{18} G, the condensate could remain favored even in hot NSs. For example, Fig. 2 shows that at 5×10^{18} G and at densities 8–10 times n_s, MDCDW could survive up to temperatures of about 40 MeV; this result could be relevant to short-lived remnant NSs of binary neutron star (BNS) merger events.

3.3. Role of topology and the β coefficients

We mentioned above how the β coefficients in (11) contain information about the topology of the MDCDW phase, and that they vanish in the absence of a magnetic field. To see their influence on the results shown in Figs 1–3, suppose the free energy is minimized at order parameters (m_0, b_0), where m_0 is small and b_0 is large. The quantity $\partial\Omega/\partial(m^2)\big|_{m=0}$ should be negative and minimized at approximately $b = b_0$. Using a 20th-order GL expansion, we have

$$\partial\Omega/\partial(m^2)\big|_{m=0} = \alpha_{2,0} + \alpha^{(20)}_{\text{inhom}} + \beta^{(20)}_{\text{inhom}}, \tag{12}$$

where

$$\alpha^{(20)}_{\text{inhom}} = \alpha_{4,2}b^2 + \alpha_{6,4}b^4 \cdots + \alpha_{20,18}b^{18} \tag{13}$$

$$\beta^{(20)}_{\text{inhom}} = \beta_{3,1}b + \beta_{5,3}b^3 \cdots + \beta_{19,17}b^{17}. \tag{14}$$

The quantity appearing in (12), evaluated at b_0, gives a rough indication of the size of m_0, with more negative values of $\partial\Omega/\partial(m^2)\big|_{m=0}$ corresponding to larger values of m_0. This quantity is plotted in Fig. 4, both omitting the contribution from the β coefficients (black curves in Fig. 4) and including it (blue curves in Fig. 4). If we did not take the β coefficients into account, the

condensate would vanish over the entire region of μ where the black curves in Fig. 4 are positive. Including these coefficients, which contain information about the phase's topology, these curves are pushed fully into the negative region (blue curves in Fig. 4), corresponding to $m > 0$, even at a temperature of 15 MeV (blue dashed curve).

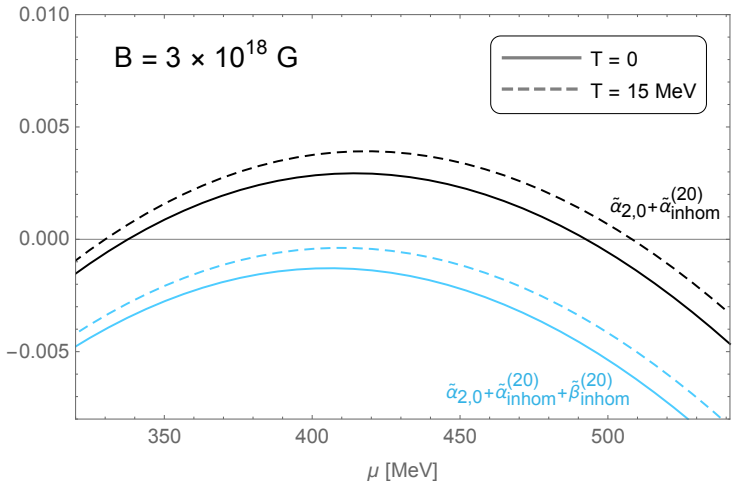

Figure 4. Combinations of GL coefficients that affect the condensate magnitude. More negative values of the curves correspond to larger m, and positive values correspond to $m = 0$. If the β coefficients are omitted (black curves), the condensate vanishes over a wide range of μ (region where black curves are positive). Including the β coefficients, we have $m > 0$ at all μ (because blue curves are always negative).

The β coefficients also play a major role in the thermal stability of the condensate. Typically, single-modulated phases in $3 + 1$ dimensions are unstable against thermal fluctuations at any arbitrarily small finite temperature, a phenomenon known as the Landau-Peierls (LP) instability [15]. It has been recently shown, however, that the presence of a magnetic field removes this instability from the MDCDW phase [14]. Using the GL expansion, the average fluctuation size can be expressed as a certain combination of the GL coefficients, and the resulting quantity is seen to be divergent at any $T > 0$ precisely when the β coefficients vanish. The asymmetry of the LLL, which causes the β coefficients to be nonzero, is therefore related to the absence of the LP instability from the condensate.

We have described several physical features of MDCDW that can be associated with the system's nontrivial topology, which is in turn related to the asymmetry of the LLL modes. Given the simplicity of the ansatz (2), it is remarkable that such a rich theory emerges, whose properties arise from a complex combination of physical mechanisms. We summarize the role of the theory's topology and its consequences in Fig. 5.

4. Conclusion

The MDCDW condensate is a robust candidate phase for the description of cold, dense quark matter in a magnetic field. In fields greater than 2×10^{18} G, the condensate remains favored over the chirally symmetric ground state at all densities, up to temperatures a few times 10 MeV. In smaller fields, say a few times 10^{17} G, the condensate is still favored over a wide range of parameter space, including temperatures consistent with cold neutron stars. Therefore, not only do we find the answer to this paper's title question—whether MDCDW can survive the temperature of a cold neutron star—to be a likely "yes," but it even seems feasible that the

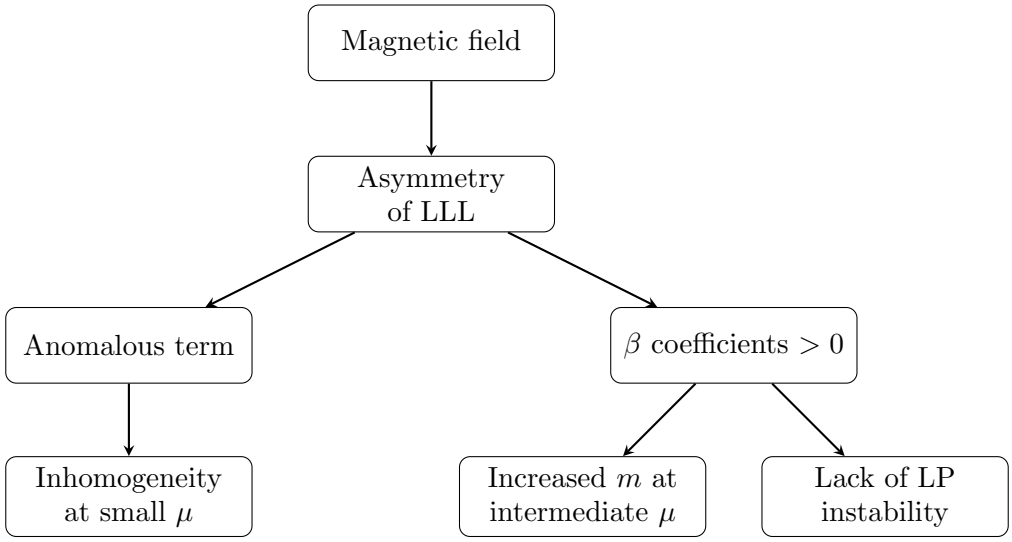

Figure 5. Concept map showing how the topology of MDCDW affects its physical characteristics.

condensate could be present in hot neutron stars, such as the young remnants of BNS mergers, provided the magnetic fields are strong enough.

MDCDW has also passed several other tests related to its viability as a candidate for compact star matter. Recent work has shown that the LP instability is absent from this phase due to topological effects related to the asymmetry of the LLL modes, so the condensate is not effectively erased by thermal fluctuations [14]. The condensate's heat capacity [16] is consistent with observational constraints [17], and the maximum stellar mass of a hybrid star whose core consists of a variant of MDCDW [18] is also compatible with astrophysical data [19]. We hope that future research on this condensate will continue to shed light on its possible relevance to compact stars and the physics of strongly interacting matter.

5. Acknowledgments

The results presented in this paper were based on work done in collaboration with Vivian de la Incera and supported in part by NSF Grant No. PHY-2013222. I am also grateful to UTRGV for monetary support during a portion of this research.

References

[1] Buballa M and Carignano S 2015 *Prog. Part. Nucl. Phys.* **81** 39 (arXiv:1406.1367)
[2] Fulde P and Ferrell R A 1964 *Phys. Rev.* A **135** 550
Larkin A I and Ovchinnikov Y N 1964 *Zh. Eksp. Teor. Fiz.* **47** 1136; 1965 *Sov. Phys. JETP* **20** 762
[3] Maeda K, Hatsuda T and Baym G 2013 *Phys. Rev.* A **87** 021604 (arXiv:1205.1086)
Roscher D, Braun J and Drut J E 2014 *Phys. Rev.* A **89** 063609 (arXiv:1311.0179)
[4] Overhauser A W 1960 *Phys. Rev. Lett.* **4** 415
[5] Brown G E and Weise W 1976 *Phys. Rep.* **27** 1
Migdal A B 1978 *Rev. Modern Phys.* **50** 107
Migdal A B 1971 *Zh. Eksp. Teor. Fiz.* **61** 2209
Migdal A B 1973 *Phys. Rev. Lett.* **31** 257
[6] Deryagin D V, Grigoriev D Y and Rubakov V A 1992 *Internat. J. Modern Phys.* A **7** 659
[7] Kutschera M, Broniowski W and Kotlorz A 1990 *Phys. Lett.* B **237** 159
[8] Nakano E and Tatsumi T 2005 *Phys. Rev.* D **71** 114006 (arXiv:hep-ph/0411350)
Nickel D 2009 *Phys. Rev.* D **80** 074025 (arXiv:hep-ph/0906.5295)
Nickel D 2009 *Phys. Rev. Lett.* **103** 072301 (arXiv:0902.1778)

[9] Kojo T, Hidaka Y, McLerran L and Pisarski R D 2010 *Nucl. Phys.* A **843** 37 (arXiv:0912.3800)
[10] Alford M G, Schmitt A, Rajagopal K and Schäfer T 2008 *Rev. Mod. Phys.* **80** 1455 (arXiv:0709.4635)
[11] Frolov I, Zhukovsky V and Klimenko K 2010 *Phys.Rev.* D **82** 076002 (arXiv:1007.2984)
[12] Ferrer E J and de la Incera V 2018 *Nucl. Phys.* B **931** 192–215 (arXiv:1512.03972)
[13] Gyory W and de la Incera V 2022 *Phys. Rev.* D **106** 016011 (arXiv:2203.14209)
[14] Ferrer E J and de la Incera V 2020 *Phys. Rev.* D **102** 104101 (arXiv:1902.06810)
[15] Peierls R 1934 *Helv. Phys. Acta* **7** 81; 1935 *Ann. Inst. Henri Poincare* **5** 177
Landau L D 1937 *Phys. Z. Sowjetunion* **11** 26; 1937 *Zh. Eksp. Teor Fiz.* **7** 627
Hidaka Y, Kamikado K, Kanazawa T and Noumi T 2015 *Phys. Rev.* D **92** 034003 (arXiv:1505.00848)
Lee T-G, Nakano E, Tsue Y, Tatsumi T and Friman B 2015 *Phys. Rev.* D **92** 034024 (arXiv:1504.03185)
Pisarski R D, Shokov V V and Tsvelik A M 2019 *Phys. Rev.* D **99** 074025 (arXiv:1801.08156)
[16] Ferrer E J, de la Incera V and Sanson P 2021 *Phys. Rev.* D **103** 123013 (arXiv:2101.04032)
[17] Cumming A, Brown E F, Fattoyev F J, Horowitz C J, Page D and Reddy S 2017 *Phys. Rev.* C **95** 025806 (arXiv:1608.07532)
[18] Carignano S, Ferrer E J, de la Incera V and Paulucci L 2015 *Phys. Rev.* D **92** 105018 (arXiv:1505.05094)
[19] Demorest P, Pennucci T, Ransom S M, Roberts M S E and Hessels J W T 2010 *Nature* **467** 1080–83 (arXiv:1010.5788)
Arzoumanian Z *et al* 2018 *Astrophys. J. Suppl.* **235** 37 (arXiv:1801.01837)
Antoniadis J *et al* 2013 *Science* **340** 6131 (arXiv:1304.6875)